Stability and electronic structure of Si, Ge, and Ti substituted single walled carbon nanotubes

Annia Galano[1] and Emilio Orgaz[2]
[1]*Instituto Mexicano del Petróleo, Eje Central Lázaro Cárdenas 152, Codigo Postal 07730, México, Distrito Federal, México*
[2]*Departamento de Física y Química Teórica, Facultad de Química, Universidad Nacional Autónoma de México, Codigo Postal 04510, México, Distrito Federal, México*
(Received 16 August 2007; published 11 January 2008)

Si, Ge, and Ti substituted nanotubes have been theoretically investigated. We employed a mixed approach for the computation of the electronic structure of these systems under periodic conditions. Band energy methods were then employed at a pseudopotential and all-electron schemes. The optimized geometries, binding, and atom-substitution energies have been computed along with the details of the electronic structure and bonding characteristics. Our results indicate the feasibility of up to now hypothetical Ge and Ti large substitutions in single walled carbon nanotubes. We also discuss the electronic behavior and the nature of the bonding in this class of materials.

DOI: 10.1103/PhysRevB.77.045111 PACS number(s): 73.22.−f, 61.46.Fg

I. INTRODUCTION

The great appeal of carbon nanotubes lies in their unique properties, which have opened a wide range of potential applications for these fascinating structures. One way to expand their applicability, and at the same time make them more efficient for specific purposes, is through structural modifications of the carbon lattice.[1–6] Generally speaking, there are two main research directions involving nanomaterials: to study the properties of existing structures and to design new materials aiming for specific properties. In the second direction, several research groups tried either to synthesize new nanotubes based on elements other than carbon[7–9] or to theoretically model hypothetic tubes.[10] In both cases, the first candidate to substitute carbon was silicon. Various silicon-carbon nanostructures (SiC-NTs), such as nanoparticles,[11] nanorods,[7,12,13] nanowires,[14–17] nanobelts,[18] nanotubes,[8,9,19,20] nanocables,[21–23] and hollow spheres,[24–26] have been successfully prepared. The presence of Si atoms changes their physical properties and chemical behavior. Consequently, the study of the influence of such defects on their properties could be relevant to eventual applications of such compounds. To our best knowledge, there are no reports on the production of GeC-NT or TiC-NT. However, there is no apparent reason to rule out the viability of such structures. Computational modeling has proved to be a useful tool in the description of new and even hypothetical materials. For instance, the conductivity properties of single walled carbon nanotubes (SWCNTs) and its dependence on the diameter and the chirality of the hexagonal lattice along the tubes were theoretically predicted by Mintmire *et al.*,[27] before SWCNTs were experimentally discovered. The increasing interest in SiC nanostructures arises from their exceptional properties such as thermal stability, high thermal conductivity, and high reactivity of the surface among others,[15,28] which make them ideal candidates for nanodevices that operate in harsh environments.[21] It is well known that C and Si have different bonding characteristics, despite the fact that they belong to the fourth chemical family and, accordingly, they have the same number of valence electrons. For instance, graphite is the more stable phase of carbon, while an equivalent phase has never been experimentally observed for silicon. Specially in clusters, carbon forms stable linear chains and planar and cage structures (sp^2 hybridization)[29,30] while silicon clusters prefer three-dimensional structures.[31,32] In contrast, there is a great similarity between silicon and germanium regarding their structural and electronic properties. Ge also forms three-dimensional structures with tetrahedrally coordinated atoms. Therefore, even though there are no experimental reports on successful synthesis of GeC nanostructures, it seems reasonable to assume that they are equally likely to be formed. Concerning TiC nanostructures, the existence of Ti_8C_{12} fullerene-like structures has been proven.[33] Neutral titanium, with its four valence electrons, was viewed as being *carbon-like* in the cage structure of a pentagonal dodecahedron, which then became isostructural, isoelectronic, and, with some restriction, isolobal with the C20 icosahedron,[34] due to the presence of *d* orbitals. However, the nature of the electronic structure of both elements is strongly different. Accordingly, it seems reasonable to assume the viability of TiC nanotubes. Since pristine carbon nanotubes may present metallic or semiconductor behavior depending on their chirality,[35–39] it seems relevant to investigate the effect of different chemical substitutions on their electronic properties prior to being considered as nanoelectronic device materials. Thus, in this work, we have studied the influence of Si, Ge, and Ti substitutions in carbon nanotubes. We computed the electronic structure of a large variety of substituted nanotubes within an energy band approach. We determined the equilibrium geometries and derived the binding and atom-substitution energies and the electronic structure for these modified structures.

II. METHODOLOGY

Due to the large unit cells exhibited by the different structures under investigation, we employed a two step approach. In the first step, we carried out computations of the electronic structure by means of a suitable pseudopotential scheme. Geometry optimizations of the different proposed substituted systems were obtained within this methodology. Thus, geom-

TABLE I. Diameters (Å), number of atoms per unitary cell, and orthorhombic lattice parameters (Å) of the studied pristine nanotubes. Results obtained at GGA/PW91/DND theory level.

Tubes	Diameter	Atoms/cell	a	b	c
(4, 4)	5.35	32	15.77	15.77	4.92
(5, 5)	6.68	40	18.21	18.21	4.98
(6, 6)	7.96	48	20.43	20.43	5.00

etry optimizations were obtained for all the modeled systems, under periodic boundary condition, within the framework of density functional theory (LDA) as implemented in the DMOL3 code,[40,41] through the Material Studio user interface. We use effective core potentials[42,43] with double numerical plus d-functions basis set (DND). Single point calculations using the Perdew-Wang[44] (PWC) generalized gradient approximation (GGA), and the same basis sets, were performed at the previously optimized geometries to improve the total energy results. In a second step, *ab initio* all-electron solid-state electronic structure calculations of (5,5) armchair pristine and selected substituted nanotubes were carried out using a density functional theory approach to band theory, employing the full potential linear augmented plane waves (LAPW) method (WIEN2K code).[45] In this full periodic approach, the nanotubes were modeled by introducing empty space in the radial direction. The closest interatomic distance between adjacent nanotubes was set to 16 Å. This distance guarantee a negligible interaction between nanotubes. The exchange part of the crystal potential was modeled by means of the generalized gradient approximation[46] to the local density. For these LAPW computations, we selected 36 **k** points in the irreducible wedge of the small orthorhombic Brillouin zones. The *muffin-tin* radii were fixed to 1.25 a.u. for C, Si, and Ge and to 1.7 a.u. for Ti atoms. The total density of states (DOS) as well as the angular momentum resolved density of states (PDOS) at each atomic site were computed by the standard tetrahedra integration scheme with a Gaussian ($\delta\epsilon$=0.05 eV) broadening. In order to test the consistency of both approaches, geometry optimization of the crystal structures was obtained for the (5,5) and (5,5)SiC-NT with 2.5% Si by refining the atomic site positions obtained in the previously optimized structures at a lower level of theory. The convergence criteria were set to 10^{-3} Ry in the total electronic energy and 2 mRy/a.u. for the local forces. Similar geometries were obtained from both approaches.

III. RESULTS AND DISCUSSION

A. Geometry optimizations and stability: Armchair structures

There are two types of bonds in infinite pristine armchair nanotubes, one perpendicular to the tube axis and another one partially along the axis. The corresponding bond distances have been represented as r_1 and r_2, as described by Dresselhaus *et al.*[47] For all the studied cases, r_1 was found to be larger than r_2 in the fully optimized geometries. The largest bond length differences ($\Delta_{1-2}=r_1-r_2$) were found to be

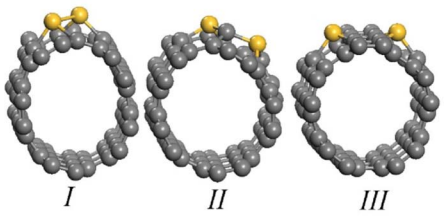

FIG. 1. (Color online) Optimized geometries of (5,5) nanotubes substituted with two silicon atoms.

0.03 Å for the (4,4) carbon nanotube (CNT), and equal to 0.02 for the other tubes. The different pristine tubes studied in this work, together with their diameters and number of atoms included in the unitary cell, are shown in Table I. It also shows the optimized lattice parameters used to define the cell dimensions: a, b, and c, with c parallel to the tube axis. The diameters reported in this table were calculated as $D=d_{CC}\frac{\sqrt{3}}{\pi}\sqrt{n^2+m^2+nm}$, where d_{CC} represents the nearest-neighbor C-C distance (r_i) in each tube, and $n=m$ for armchair nanotubes.[47]

Different structural modifications have been studied by replacing C atoms of the carbon lattice with Si, Ge, or Ti (X) in various X/C ratios. For unit cells with two X atoms, three different isomers have been tested for the (5,5) tube, with the substitutions of two carbon centers in the same hexagonal ring. Figure 1 shows the corresponding structures for X=Si as illustration. In structure I, the X centers are next to each other (ortho), while in structures II and III, they are separated by one (meta) or two (para) carbon atoms, respectively. We have only considered double Si substitution in the same ring, since Mavrandonakis *et al.*[48] have found that other double substitutions (involving different hexagons), although possible, are less energetically favored. The electronic energies of the optimized structures and the X-X bond lengths are shown in Table II. It should be noticed that, in this case, the unitary cell was modeled using 80 atoms to avoid unwanted interactions between X atoms. Isomers III were found to be the most energetically favored, regardless of the dopant's nature. Based on this finding, all the other nanotubes with two X atoms, per unitary cell, were modeled using a similar distribution, i.e., with the two X separated by two C atoms. For the CNT 50% substituted, we only consider type-1 structures as defined by Menon *et al.*[49,50] These authors reported that the type-2 structures are systematically less stable by around 0.4 eV per CSi pair.

TABLE II. Electronic energies and $X-X$ bond lengths (Å) for double substituted (5,5) nanotubes (X=5%). Results obtained at GGA/PW91/DND theory level.

	Energy			$d(X-X)$	
X	I	II	III	I	II
Si	−7038.88	−7038.92	−7038.94	2.36	3.08
Ge	−14273.31	−14273.45	−14273.50	2.66	3.36
Ti	−9290.12	−9289.74	−9290.13	2.83	3.25

TABLE III. Selected geometrical parameters of X-substituted (5,5) nanostructures (Å), and binding and atom-substitution energies (eV). Results obtained at GGA/PW91/DND theory level.

		d(C-C)[a]	d(C-X)[b]					
	% X	r_1	r_2	r_1	r_2	$d(X-X)$[c]	BE	E_{subst}
C_{40}	0	1.40	1.42				−8.33	
$C_{39}Si$	2.5	1.39	1.40	1.86	1.76		−8.20	5.36
$C_{38}Si_2$	5	1.38	1.40	1.85	1.76	3.58	−8.06	5.49
$C_{36}Si_4$	10	1.42	1.40	1.85	1.78	3.51	−7.78	5.55
$C_{34}Si_6$	15	1.42	1.45	1.85	1.78	3.45	−7.51	5.45
$C_{32}Si_8$	20	1.40	1.51	1.82	1.94	3.15	−7.27	5.33
$C_{20}Si_{20}$	50			1.80	1.79	3.09	−6.07	4.52
$C_{39}Ge$	2.5	1.39	1.40				−8.15	7.34
$C_{38}Ge_2$	5	1.41	1.39	2.02	1.94	4.01	−7.97	7.15
$C_{36}Ge_4$	10	1.41	1.40	2.03	1.92	3.82	−7.61	7.2
$C_{34}Ge_6$	15	1.40	1.37	2.03	1.93	3.54	−7.27	7.09
$C_{32}Ge_8$	20	1.41	1.36	2.04	1.97	3.20	−6.97	6.83
$C_{20}Ge_{20}$	50			1.87	1.83	3.25	−5.24	6.19
$C_{39}Ti$	2.5	1.40	1.41	1.97	1.95		−8.2	5.19
$C_{38}Ti_2$	5	1.39	1.41	1.96	1.95	4.08	−8.06	5.41
$C_{36}Ti_4$	10	1.39	1.41	1.95	1.95	4.19	−7.76	5.71
$C_{34}Ti_6$	15	1.42	1.43	2.07	2.00	3.73	−7.50	5.53
$C_{20}Ti_{20}$	50			1.94	1.91	3.06	−5.92	4.82

[a]In the vicinity of the X atoms.
[b]Average values.
[c]For the closest $X-X$ pair.

Table III shows selected geometrical parameters of the X-substituted (5,5) nanostructures. In all cases, subscripts 1 and 2 keep the meaning explained above, related to the orientation of the bonds with respect to the tube's axis. Two energetic parameters have been used to evaluate the relative stability of the different tubes and have also been included in this table. The first one is the binding energy (BE) per atom, with respect to dissociation into elements, which has been calculated as $BE_{XCNT}=(E_{XCNT}-n_C E_C-n_X E_X)/(n_X+n_X)$, where n_C and n_X account for the number of C and X atoms in the tube. E_C and E_X represent the electronic energies of C and X atoms, and E_{XCNT} stands for the electronic energy of the substituted tube. The pristine CNTs have also been considered for comparison purposes. The second parameter is the energetic cost associated with the replacement of a C atom by an X atom in the nanotube. We are referring to this energetic parameter as atom-substitution energy (E_{subst}) according to the hypothetical reaction $C_{CNT}+X\rightarrow C_{XCNT}+C$, and it has been calculated as $E_{subst}=(E_{XCNT}+n_C E_C-E_{CNT}-n_X E_X)/n_X$.

The values in Table III were obtained from structures optimized at LDA/PWC/DND level of theory and, using these geometries, the energy values were improved by single point calculations at GGA/PW91/DND level. As should be expected, from the electronic distribution of the corresponding atoms, the C-Si distances are shorter than the C-Ge and C-Ti. In addition, the C-X distances do not appreciably change as the number of X atoms increases. According to the values on Table III, the C–C bond distances remain almost unchanged, with respect to pristine tubes, even in the vicinity of the dopants. Accordingly, it can be concluded that the deformation, caused by the inclusion of X atoms in the carbon lattice, is essentially local. It seems relevant to notice that as the X/C ratio increases the energetic cost, per atom of replacing C by X, decreases when going from 2.5% to 50% of X. However, there is an apparent increase in this cost for tubes with about 10% of X. Accordingly, it can be hypothesized that these XCNTs might be especially difficult to achieve. In addition, the atom-substitution energy associated with Ge is appreciably larger (about 2 eV) than those for equivalent X/C ratios where the carbon lattice has been substituted with Si or Ti. Thus, it seems reasonable to assume that the production of GeC-NTs would be more challenging, or at least it should take place at significantly higher temperatures, than the production of SiC-NTs and TiC-NTs.

For the binding energies, a clear trend was observed: the BE decreases as the X/C ratio increases. This is an expected behavior. The pristine tube can be considered as an infinite folded graphene sheet, i.e., infinite conjugated π system, with a huge electron delocalization involving all the atoms in the sheet since they all have sp^2 hybridization. This delocalization represents an extra stabilization of the chemical bonds and lowers the binding energy, compared to a nonconjugated system. This effect is maximum for planar sheets and decreases as the CNTs become thinner, since, as the curvature of the tube increases, the C atom's configuration is farther from the ideal sp^2. On the other hand, when Si, Ge, or Ti defects appear in the carbon lattice, this conjugation is broken by the inclusion of an atom that leads to three-

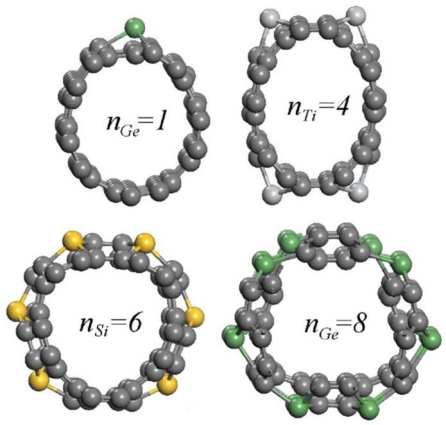

FIG. 2. (Color online) Optimized geometries of selected substituted tubes, showing the number of X atom per unitary cell.

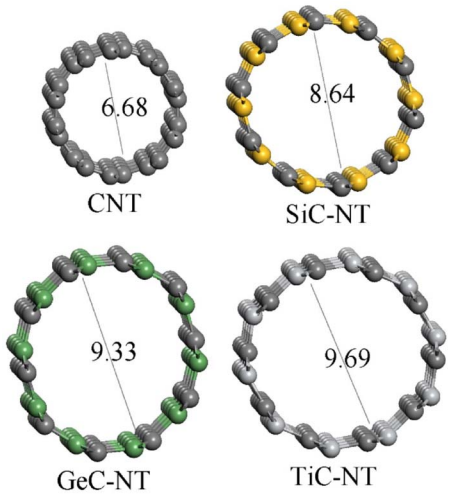

FIG. 3. (Color online) Optimized structures of substituted carbon nanotubes at X=50% and their approximated diameters.

dimensional, shoulderlike, perturbations (Fig. 2). It seems interesting that the presence of Si or Ti in the carbon lattice has equivalent effects on the binding energy, while Ge has a larger destabilizing effect. The presence of each X atom not only disrupts the conjugated system, but also locally deforms the surface of the tube, which increases its curvature at the X centers. This deformation becomes less relevant as the X/C ratio increases. We have used the dihedral angle between each X atom and the plane formed by the three carbon atoms bonded to it as a measurement of the extent of such deformation. The corresponding values are reported in Table IV, which also includes the equivalent dihedral angles for the pristine tubes. As this table shows, the dihedral angle $\angle$CCCX decreases as the X/C ratio increases, approaching the value of the pristine tube. Since the diameter of the tubes also increases with the X/C ratio, the values of $\angle$CCCX for XCNT structures with 50% X can become even lower than that of the pristine tube. For this X:C proportion, the walls of the tubes show a smooth shape, without any local shoulder (Fig. 3).

For silicon substitution in the carbon lattice, the modeling has been extended to tubes of different diameters. In these cases, unitary cells with one or two Si atoms have been computed as well as those with 50% of Si. Table V shows selected geometrical parameters of these compounds, together with the corresponding binding and atom-substitution energies, all of them correspond to LDA/PWC/DND theory approach. Comparing the (5,5) structures from Tables III and V, it is clear that the binding and atom-substitution energies obtained at both theory levels qualitatively agree. We summarize these results in Fig. 4. The binding energies shown in Table V and Fig. 4 become more negative as the diameter of the tube increases. This result is in line with the above discussion. For the atom-substitution energies, the tendency exhibited by the (5,5) XCNTs is maintained for (4,4) and (6,6) derived tubes. The energetic cost of replacing C by X decreases as the X/C ratio increases.

TABLE IV. Average values of the CCCX dihedral angles in substituted (5,5) nanotubes. Results obtained at GGA/PW91/DND theory level.

	% X	X=Si	X=Ge	X=Ti
C_{40}	0	11.77		
$C_{39}X$	2.5	48.58	53.66	58.36
$C_{38}X_2$	5	46.63	54.70	54.70
$C_{36}X_4$	10	46.70	51.65	54.72
$C_{34}X_6$	15	40.18	49.01	49.70
$C_{32}X_8$	20	26.17	30.09	34.79
$C_{20}X_{20}$	50	10.18	8.52	21.64

In Fig. 5, we plot the estimated structure volume as a function of the substitution percentage for the (5,5) derived systems. The volumes were estimated using the van der Waals radii for each atom. As can be appreciated in the figure, the Si substitution has a stronger deformation effect in the nanotube compared with Ge and Ti substitutions. This is a testimony of the resistance of Si to accept environments far from the tetrahedral one. However, Ge and Ti can accommodate in a better way these local deformations, avoiding a pronounced increase of the structure volume. It is interesting to note that at X/C ratio of 20%, clearly a strong increase in the cell volume and a change in the rough linear behavior are observed at lower X/C substitutions. This change in the cell volume behavior is also evident for the Ge and Ti substituted nanotubes, but in a small extent.

B. Electronic structure analysis

In Fig. 6(a), we plotted the total DOS for the (5,5) pristine nanotube along with that obtained for the (5,5)Si 2.5% substituted structure. This plot permits directly comparing both DOS and observing the effect of the Si substitution at the lowest X:C ratio investigated. In the (5,5) SiC-NT with 2.5% Si, the Si-Si distance is 4.9 Å and can be roughly considered as a diluted substitution case. The effect of Si substitution clearly appears in this plot, introducing new Si p states, in particular, close to the Fermi energy (E_F). Our results are consistent with recent results of Titantah *et al.*[51] and Avra-

TABLE V. Selected geometrical parameters of Si-substituted nanostructures (n,m) (Å), and binding and atom-substitution energies (eV). Results obtained at LDA/PWC/DND theory level.

(n,m)	nSi	% Si	d(C-C)[a] $r1$	$r2$	d(C-Si) $r1$	d(Si-Si)[b] $r2$		BE	E_{subst}
(4,4)	0	0	1.40	1.42				−9.21	
	1	3.1	1.40	1.40	1.89	1.77		−9.01	6.24
	2	6.3	1.38	1.40	1.89	1.78	3.70	−8.84	5.80
	8	25	1.41	1.48	1.84	1.99	3.21	−7.90	5.25
	16	50			1.80	1.79	3.08	−6.63	5.15
(5,5)	0	0	1.40	1.42				−9.30	
	1	2.5	1.39	1.40	1.86	1.76		−9.14	6.14
	2	5	1.38	1.40	1.85	1.76	3.58	−8.99	6.08
	8	20	1.40	1.51	1.82	1.94	3.15	−8.10	5.98
	20	50			1.89	1.79	3.09	−7.28	4.03
(6,6)	0	0	1.39	1.43				−9.38	
	1	2.1	1.39	1.40	1.84	1.76		−9.20	5.71
	2	4.2	1.38	1.41	1.84	1.77	3.56	−9.07	5.99
	8	16.8							
	24	50			1.80	1.79	3.10	−6.73	5.18

[a]In the vicinity of the X atoms.
[b]The shortest $X-X$ distance.

mov *et al.*[52] In Fig. 6(b), we show the PDOS at the Si site and at an adjacent C atom (C_{adj}). It is clear that the C_{adj}-Si interaction is strong in this energy range. The contribution to the DOS from C atoms far (C_{far}) from the Si site (not bounded to Si) resembles that of the C atoms in the pristine nanotube. This means that the Si substitutions have only a local effect. In order to support this, Fig. 6(c) shows the PDOS difference between C_{adj} and C_{far}. As can be appreciated, a high density of C p states is concentrated close to the E_F for the C_{adj}. This is a testimony of the particular Si-C chemical bond in this nanotube.

The effect of larger substitutions on the DOS structure is, in general, complex. When the Si content increases, the Si-Si interaction gets stronger and the effect of the Si p states, close to the E_F, becomes more important. In Fig. 7(a), we plotted the total DOS for the (5,5) Si 5%, where two Si atoms are contiguous (*ortho* position). Below the Fermi energy, the number of Si p states increases, broadening the structure in such a way that only four well defined peaks

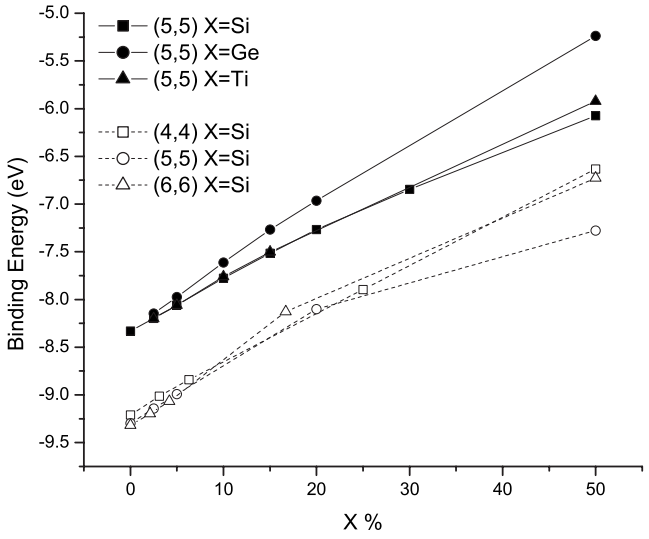

FIG. 4. Binding energies per atom (eV) for different X/C ratios. Solid lines (dark symbols) were obtained at GGA/PW91/DND, and dashed lines (open symbols) at LDA/PWC/DND theory levels.

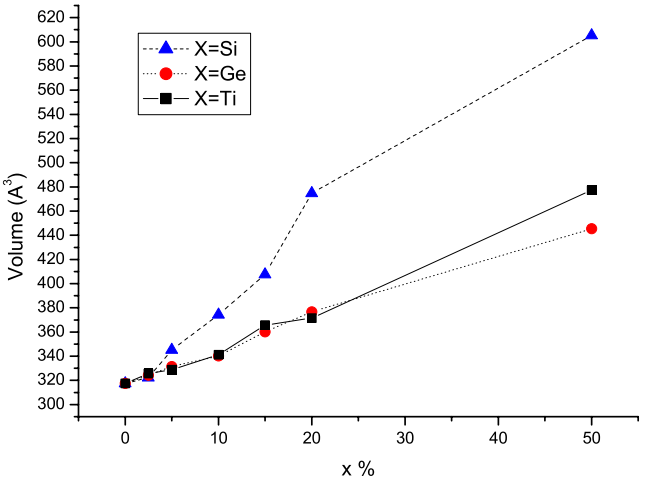

FIG. 5. (Color online) Structure volume (Å^3) computed with van der Waals radii of the elements for different substituted nanotubes as a function of the substitution percentage.

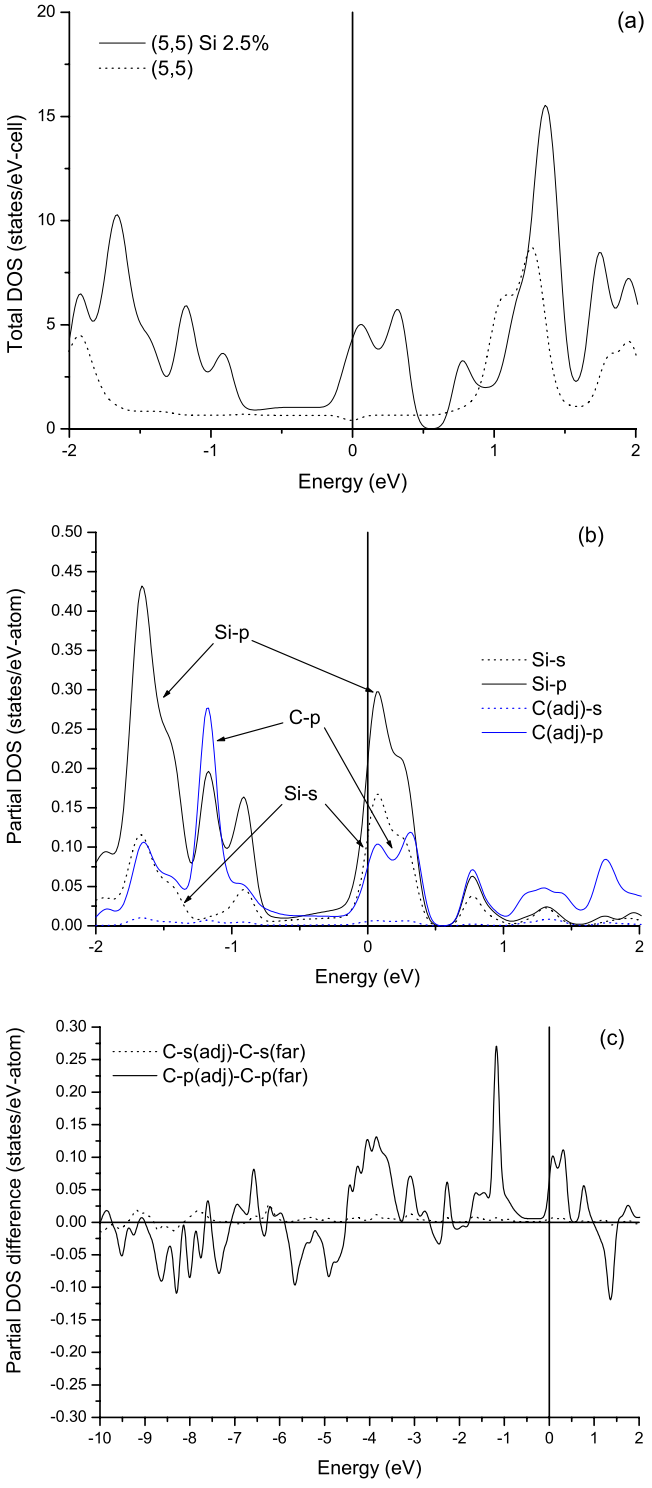

FIG. 6. (Color online) (a) Total DOS (states/eV 40-atom cell) for the 2.5% Si-substituted (5,5) carbon nanotube, and the corresponding (5,5) pristine nanotube, (b) partial DOS (states/eV atom) at the Si and adjacent C sites. (c) Partial DOS differences ($C_{adj}-C_{far}$). Fermi energy was set to zero. Results obtained at LAPW theory level.

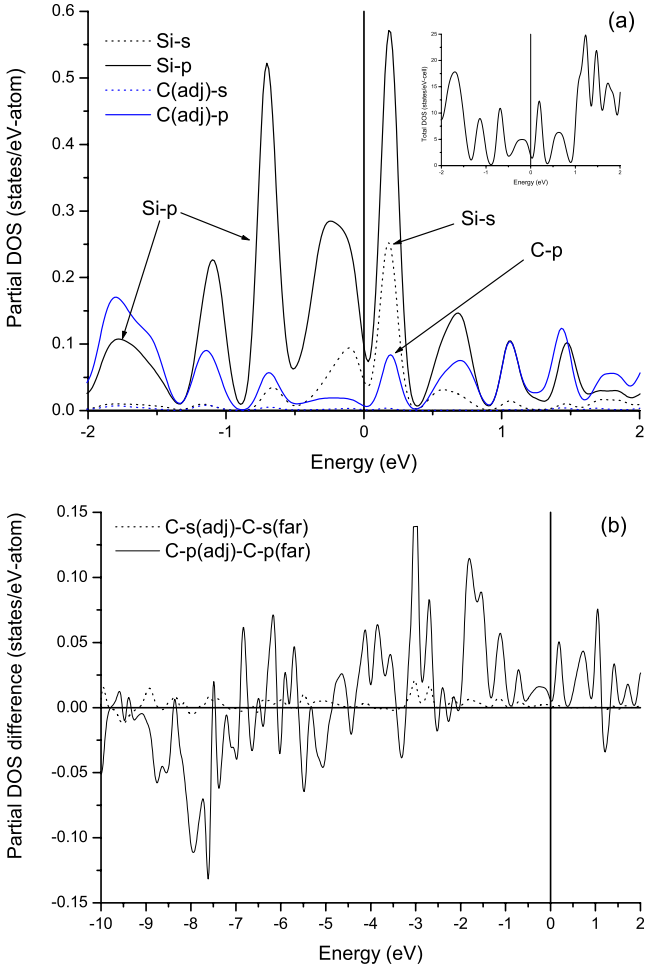

FIG. 7. (Color online) (a) Partial DOS (states/eV atom) at the Si and adjacent C sites for the 5% Si-substituted (5,5) carbon nanotube (*ortho* configuration). In inset, the total DOS (states/eV 80-atom cell) and (b) partial DOS differences ($C_{adj}-C_{far}$). Fermi energy was set to zero. Results obtained at LAPW theory level.

appear. The broad peak appearing in the DOS at −0.25 eV is strongly dominated by the Si *p* orbitals. This can be appreciated in the detailed PDOS of Fig. 7(a). In this plot, we included also the C_{adj} contributions. The DOS peak at 0.3 eV above the E_F is also an effect of Si substitutions. The DOS contribution unbalanced between C_{adj} and C_{far} atoms is again clear in Fig. 7(b). C_{adj} exhibits a strong contribution of *p* states close to the Fermi energy. In these plots, the broadening of the DOS (and PDOS) masks the semiconducting behavior predicted for the Si 5% substituted nanotube in the *ortho* and *meta* configurations. The total energy computations discussed in the previous section indicate that the more stable form is the *para* configuration, which appear to be metallic as expected. This interesting behavior and then the predictive ability of the density functional theory (DFT) methods will be found again for the Ge-based systems commented below. However, some inconsistencies on the metallic or semiconducting behavior predicted by DFT methods have been detected depending on the DFT approach,[53] in particular, for small radii NTs.

For simplicity, we will skip the details of the results for intermediate Si substitution ratios. However, the 50% substitution case deserves more attention. Here, unambiguously, the structure becomes insulating.[54,55] Our estimation

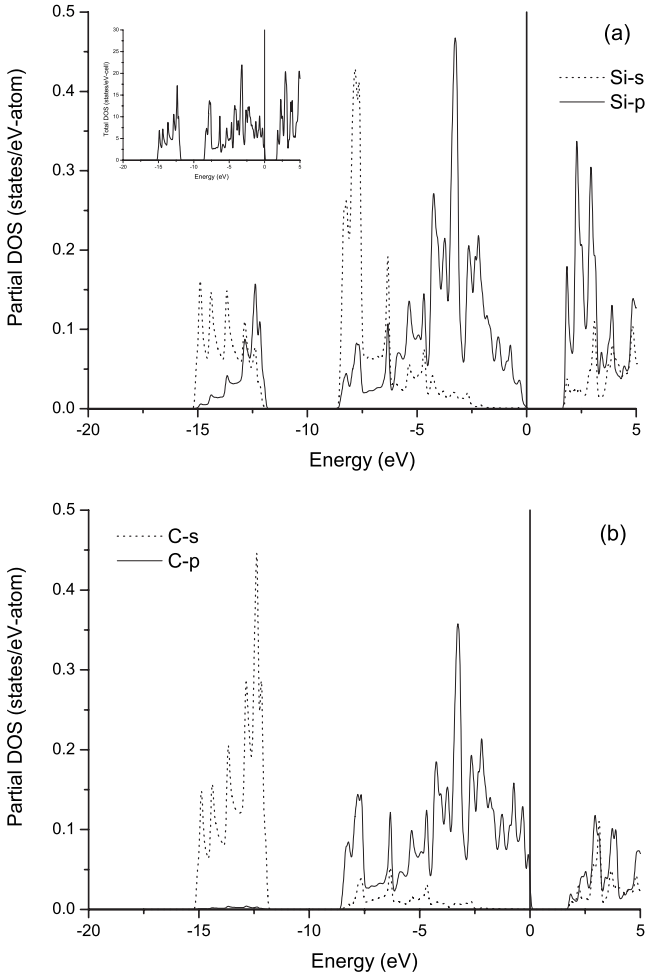

FIG. 8. (a) Partial DOS (states/eV atom) at the Si site for the 50% Si-substituted (5,5) carbon nanotube. In inset, the total DOS (states/eV 20-atom cell) and (b) partial DOS (states/eV atom) at the C site. Fermi energy was set to zero. Results obtained at LAPW theory level.

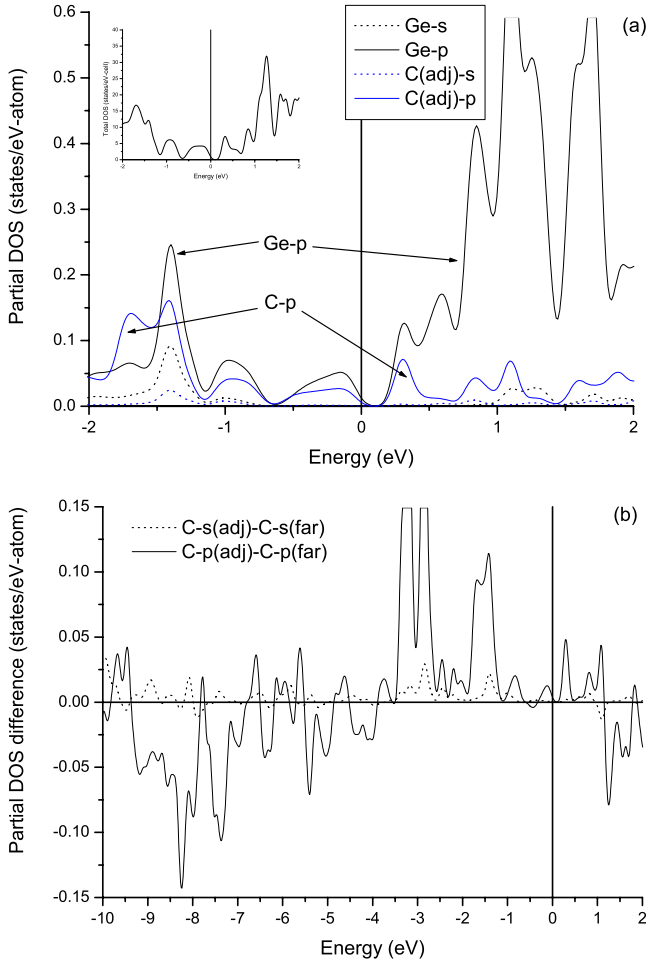

FIG. 9. (Color online) (a) Partial DOS (states/eV atom) at the Ge and adjacent C sites for the 5% Ge-substituted (5,5) carbon nanotube (*ortho* configuration). In inset, the total DOS (states/eV 80-atom cell) and (b) partial DOS differences ($C_{adj}-C_{far}$). Fermi energy was set to zero. Results obtained at LAPW theory level.

for the energy gap is 1.7 eV. It seems that the metal-to-semiconductor transition occurs at 20% of Si substitution. This result is qualitatively consistent with the trends found in the work of Avramov *et al.*[52] who established a transition at 5% Si for (8,8)CNT and a semiconducting behavior for pristine and all the Si substituted (10,0)CNTs. It is interesting to note that a correlation exists between the metal-to-semiconductor transition and the strong structural modification represented in Fig. 5. In Fig. 8, we plotted the total DOS along with the Si and C site contributions to the DOS. We found good agreement with the results of Zhao *et al.*[54] for this system. In this structure, the C atoms are all involved in bonding with Si so the previous differentiation of C atoms does not apply. It is interesting to observe the Si *p* contribution to the DOS as a function of the Si content. The Si *p* peak appearing above the E_F changes as the Si content increases by broadening and shifting to higher energies.

The Ge-substituted (5,5) nanotubes exhibit strong similarities with the corresponding Si-substituted systems. This is not surprising based on the electronic structure of Si and Ge atoms. In Fig. 9, we plot the total and partial DOS for the (5,5) GeC-NT with 5.0% Ge. As can be appreciated, the role of the Ge *p* states close to the Fermi level is similar to that observed in the Si-based nanotubes with the same substitution ration (Fig. 7). In addition to the structural and energetic aspects discussed above, we can indicate that the metal-to-semiconductor transition occurs also close to 20% substitution ratio. The energy gap found for the (5,5)CGe-NT 50% Ge is 0.94 eV.

The Ti-substituted (5,5) compounds are fundamentally different from the view point of the electronic structure when compared to the corresponding Si or Ge structures. As previously described, the Ti atom can be easily accommodated in the (5,5) structure, but the origin of the Ti-C interactions is of a different nature. In Fig. 10, we plot the total and partial DOS for the (5,5) TiC-NT with 5.0% Ti, where two Ti atoms are contiguous (*ortho* configuration). We observe that the total DOS at the Fermi energy is particularly high when compared to the corresponding pristine (5,5) nanotube or with equivalent Si- or Ge-substituted systems. The inspection of the PDOS at the Ti site [Fig. 10(a)] makes evident the role of

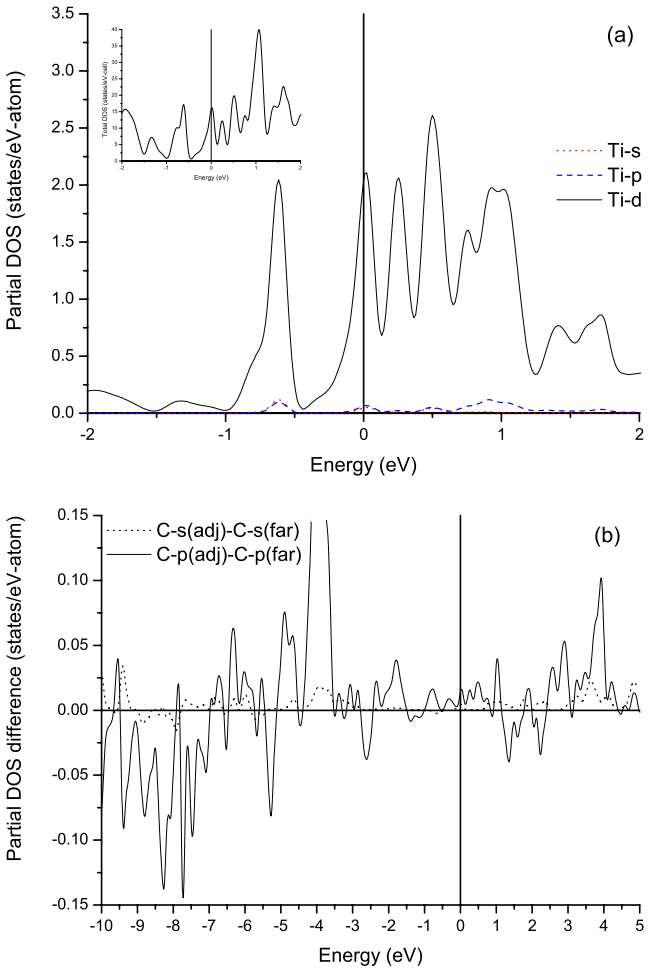

FIG. 10. (Color online) (a) Partial DOS (states/eV atom) at the Ti site for the 2.5% Ti-substituted (5,5) carbon nanotube. In inset, the total DOS (states/eV 80-atom cell) and (b) partial DOS (states/eV atom) at the C site. Fermi energy was set to zero. Results obtained at LAPW theory level.

the Ti d states in this system. Ti atom has a $3d^2 4s^2$ configuration. While the extended $4s$ orbitals can participate in direct bonding, the almost empty $3d$ localized orbitals can also contribute in direct bonding or even in a π back donating mechanism with adjacent C atoms. The Ti s contribution to the DOS is particularly small. This means that the $4s$ electrons are transferred to the host structure. In the PDOS plot at the Ti site, we observe as expected a strong contribution of Ti d orbitals localized close to E_F. Again, the more stable configuration is that having two opposite Ti atoms (*para* form). However, we found that the three configurations are metallic with a sizable DOS at the Fermi energy. The (5,5) TiC-NT with 50% Ti exhibits again a semiconducting behavior with 0.41 eV value for the energy gap.

It is interesting now to focus on the charge state of the substitution atom in the nanotube. Mülliken and natural bond order population analysis have been employed in order to determine the charge state of Si, Ge, and Ti. Usually, the obtained charge states for an atom in a molecule or solid strongly depend on the employed method. In order to verify our results, we perform Si, Ge, and Ti single (diluted) substitution in a graphite sheet. These calculations yield very similar results than those obtained for tubular structures. We found defective charge state for the Si, Ge, and Ti atoms in all the studied cases. This indicates that the substituted site is a charge acceptor (acidic site), which is of relevance if we are looking for reactivity sites in these substituted carbon nanotubes. We found that Ti($q=+2.11$) is more charge defective than Si(+1.94) and Ge(+0.95). We found a systematic increase of the total DOS at the Fermi level for substituted nanotubes with respect to the pristine (5,5) structure. For the same X/C ratio, Ti exhibits a higher increase on the total DOS at E_F with respect to the corresponding Si and Ge [see Figs. 6(a), 7(a), 9(a), and 10(a)]. For higher substitution ratios, an energy gap opens and the system becomes semiconducting. However, Si and Ge usually exhibit hypervalent compounds and it is not strange to find highly oxidized states for these atoms. The strong difference between Si and Ge deserves more attention. Si and Ge have similar electronegativities and ionization potentials. We expect a very similar behavior. However, the charge depletion is clearly more important in Si than in Ge. Ge should tend to preserve a more important covalency compared to Si and Ti.

IV. CONCLUSIONS

We have investigated Si, Ge, and Ti substitutions in a large series of armchair carbon nanotubes. We have modeled the stability, different energetic aspects, and the electronic structure of such compounds. We have found that the Ge and Ti derived compounds exhibit a more compact structure than the pristine tubes. For low X:C ratios, local deformations (shoulders) in the lattice were found at the X sites, while for 1:1 ratio, the tubes show smooth structures. The energetic cost of replacing C atoms by X was analyzed and found to be maximum for 10% substitutions, and larger for Ge than for the other studied dopants. Defective charge states were found at the Si, Ge, and Ti sites in all the investigated structures, indicating them as charge acceptor (acid) sites. The Ti-substituted compounds seem to be metallic even at large substitution ratios. The particular behavior of hypothetical Ti-substituted nanostructures stands out and makes them of potential interest to further experimental investigations.

ACKNOWLEDGMENTS

E.O. is indebted to DGSCA-UNAM for providing generous supercomputing facilities and to DGAPA-UNAM under Grant No. IN102202 for partial financial support. A.G. gratefully acknowledges the financial support from the Instituto Mexicano del Petróleo through Project No. D00446, and the IMP Computing Center for supercomputer time.

[1] V. H. Crespi, M. L. Cohen, and A. Rubio, Phys. Rev. Lett. **79**, 2093 (1997).
[2] P. G. Collins, K. Bradley, M. Ishigami, and A. Zettl, Science **287**, 1801 (2000).
[3] J. Kong, N. R. Franklin, C. Zhou, M. G. Chapline, S. Peng, K. Cho, and H. Dai, Science **287**, 622 (2000).
[4] M. Ouyang, J.-L. Huang, C. L. Cheung, and C. M. Lieber, Science **291**, 97 (2001).
[5] J. W. G. Wildöer, L. C. Venema, A. G. Rinzler, R. E. Smalley, and C. Dekker, Nature (London) **391**, 59 (1998).
[6] O. Gülseren, T. Yildirim, and S. Ciraci, Phys. Rev. B **66**, 121401(R) (2002).
[7] H. J. Dai, E. W. Wong, Y. Z. Lu, S. S. Fan, and C. M. Lieber, Nature (London) **375**, 769 (1999).
[8] C. Pham-Huu, N. Keller, G. Ehret, and M. J. Ledouxi, J. Catal. **200**, 400 (2001).
[9] X. H. Sun, C. P. Li, W. K. Wong, N. B. Wong, C. S. Lee, S. T. Lee, and B. K. Teo, J. Am. Chem. Soc. **124**, 14464 (2002).
[10] S. B. Fagan, R. J. Baierle, R. Mota, A. J. R. da Silva, and A. Fazzio, Phys. Rev. B **61**, 9994 (2000).
[11] Y. Dong and P. Molian, Appl. Phys. Lett. **84**, 10 (2004).
[12] X. T. Zhou, N. Wang, H. L. Lai, H. Y. Peng, I. Bello, N. B. Wong, C. S. Lee, and S. T. Lee, Appl. Phys. Lett. **74**, 3942 (1999).
[13] Q. Y. Lu, J. Q. Hu, K. B. Tang, Y. T. Qian, G. E. Zhou, X. M. Liu, and J. S. Zhu, Appl. Phys. Lett. **75**, 507 (1999).
[14] J. Q. Hu, Q. Y. Lu, K. B. Tang, B. Deng, R. R. Jiang, Y. T. Qian, W. C. Yu, G. E. Zhou, X. M. Liu, and J. X. Wu, J. Phys. Chem. B **104**, 5251 (2000).
[15] Z. W. Pan, H. L. Lai, F. C. K. Au, X. F. Duan, W. Y. Zhou, W. S. Shi, N. Wang, C. S. Lee, N. B. Wong, S. T. Lee, and S. S. Xie, Adv. Mater. (Weinheim, Ger.) **12**, 1186 (2000).
[16] G. Gundiah, G. V. Madhav, A. Govindaraj, M. M. Seikh, and C. N. R. Rao, J. Mater. Chem. **12**, 1606 (2002).
[17] H. J. Choi, H. K. Seong, J. C. Lee, and Y. M. Sung, J. Cryst. Growth **269**, 472 (2004).
[18] G. Xi, Y. Peng, S. Wan, T. Li, W. Yu, and Y. Qian, J. Phys. Chem. B **108**, 20102 (2004).
[19] H. Wang, X. D. Li, T. S. Kim, and D. P. Kim, Appl. Phys. Lett. **86**, 173104 (2005).
[20] L. Z. Pei, Y. H. Tang, X. Q. Zhao, Y. W. Chen, and C. Guo, J. Appl. Phys. **100**, 046105 (2006).
[21] Y. Zhang, K. Suenaga, C. Colliex, and S. Iijima, Science **281**, 973 (1998).
[22] H. F. Zhang, C. M. Wang, and L. S. Wang, Nano Lett. **2**, 941 (2002).
[23] Y. B. Li, Y. Bando, and D. Globerg, Adv. Mater. (Weinheim, Ger.) **16**, 93 (2004).
[24] C. Ray, M. Pellarin, J. L. Lerme, J. L. Vialle, M. Broyer, X. Blase, P. Melinon, P. Keghelian, and A. Perez, Phys. Rev. Lett. **80**, 5365 (1998).
[25] C. Ray, M. Pellarin, J. L. Lerme, J. L. Vialle, M. Broyer, X. Blase, P. Melinon, P. Keghelian, and A. Perez, J. Chem. Phys. **110**, 6927 (1999).
[26] Y. Zhang, E. W. Shi, Z. Z. Chen, X. B. Liab, and B. Xiao, J. Mater. Chem. **16**, 4141 (2006).
[27] J. W. Mintmire, B. I. Dunlap, and C. T. White, Phys. Rev. Lett. **68**, 631 (1992).
[28] R. Wang, D. Zhang, and C. Liu, Chem. Phys. Lett. **411**, 333 (2005).
[29] W. Andreoni, D. Scharf, and P. Giannozzi, Chem. Phys. Lett. **173**, 449 (1990).
[30] M. Menon, K. R. Subbaswamy, and M. Sautarie, Phys. Rev. B **48**, 8398 (1993).
[31] W. Andreoni and G. Pastore, Phys. Rev. B **41**, 10243 (1990).
[32] K. Raghavachari and C. M. Rohlfing, J. Chem. Phys. **94**, 3670 (1991).
[33] B. C. Guo, K. P. Kerns, and A. W. Castleman Jr., Science **255**, 1411 (1992).
[34] M. M. Rohmer, M. Benard, and J. M. Poblet, Chem. Rev. (Washington, D.C.) **100**, 495 (2000).
[35] N. Hamada, S. I. Sawada, and A. Oshiyama, Phys. Rev. Lett. **68**, 1579 (1992).
[36] S. Iijima and T. Ichihaschi, Nature (London) **363**, 603 (1993).
[37] D. S. Bethune, C. H. Kiang, M. S. de Vries, G. Gorman, R. Savoy, J. Vazquez, and R. Beyes, Nature (London) **363**, 605 (1993).
[38] Y. Miyamoto, S. G. Louie, and M. L. Cohen, Phys. Rev. Lett. **76**, 2121 (1996).
[39] B. I. Yakobson and R. E. Smalley, Am. Sci. **85**, 324 (1997).
[40] B. Delley, J. Chem. Phys. **92**, 508 (1990).
[41] B. Delley, J. Chem. Phys. **113**, 7756 (2000).
[42] M. Dolg, U. Wedig, H. Stoll, and H. Preuss, J. Chem. Phys. **86**, 866 (1987).
[43] A. Bergner, M. Dolg, W. Kuechle, H. Stoll, and H. Preuss, Mol. Phys. **80**, 1431 (1993).
[44] J. P. Perdew and Y. Wang, Phys. Rev. B **45**, 13244 (1992).
[45] P. Blaha, K. Schwarz, G. K. H. Madsen, D. Kvasnicka, and J. Luitz, *WIEN2k, An Augmented Plane* Wave+Local *Orbitals Program for Calculating Crystal Properties* (Technische Universität Wien, Austria, 2001).
[46] J. P. Perdew, K. Burke, and M. Ernzerhof, Phys. Rev. Lett. **77**, 3865 (1996).
[47] M. S. Dresselhaus, G. Dresselhaus, and A. Jorio, Annu. Rev. Mater. Res. **34**, 247 (2004).
[48] A. Mavrandonakis, G. E. Froudakis, M. Schnell, and M. Mühlhäuser, Nano Lett. **3**, 1481 (2003).
[49] M. Menon, E. Richter, A. Mavrandonakis, G. Froudakis, and A. N. Andriotis, Phys. Rev. B **69**, 115322 (2004).
[50] M. Menon, D. Srivastava, I. Ponomareva, and L. A. Chernozatonskii, Phys. Rev. B **70**, 125313 (2004).
[51] J. T. Titantah, K. Jorissen, and D. Lamoen, Phys. Rev. B **69**, 125406 (2004).
[52] P. V. Avramov, P. B. Sorokin, A. S. Fedorov, D. G. Fedorov, and Y. Maeda, Phys. Rev. B **74**, 245417 (2006).
[53] C. Kamal and A. Chakrabarti, Phys. Rev. B **76**, 075113 (2007).
[54] M. Zhao, Y. Xia, F. Li, R. Q. Zhang, and S. T. Lee, Phys. Rev. B **71**, 085312 (2005).
[55] R. J. Baierle, P. Piquini, L. P. Neves, and R. H. Miwa, Phys. Rev. B **74**, 155425 (2006).